

# Thermodynamic Interpretation of NMR Relaxation Parameters in Proteins in the Presence of Motional Correlations

J. J. Prompers and R. Brüschweiler\*

Carlson School of Chemistry and Biochemistry, Clark University, Worcester, Massachusetts 01610

Received: July 22, 2000

It is shown by quasiharmonic analysis that the conformational partition function of a globular protein sampled on the ns time scale can be factorized in good approximation into a purely reorientational part, which determines heteronuclear NMR spin relaxation, and a remaining part that includes other types of intramolecular motions. This factorization provides a statistical mechanical basis for the thermodynamic interpretation of NMR relaxation parameters of proteins where atomic motions can be significantly correlated. Reorientational entropy differences between different backbone parts of the globular protein ubiquitin are found to be remarkably insensitive to motional correlation effects, which in some cases may significantly facilitate the entropic interpretation of changes of NMR order parameters.

## 1. Introduction

Despite enormous progress toward increasingly detailed characterizations of proteins in terms of their average structures and their dynamics by a variety of experimental methods, including X-ray crystallography, NMR spectroscopy, neutron scattering, and optical spectroscopic methods, complementary thermodynamic descriptions involving enthalpy and entropy have remained valuable and appealing. While enthalpy primarily depends on the average 3D protein structure, entropy reflects the protein's mobility and its fluctuations. Direct measurements of thermodynamic quantities of proteins by calorimetric methods are possible, but these data do not give detailed insights into spatial and time-scale aspects of protein behavior.

NMR spin relaxation of  $^{15}\text{N}$  and  $^{13}\text{C}$  labeled proteins provides a wealth of information on protein dynamics with atomic resolution.<sup>1</sup> Spatial aspects of motions that affect relaxation parameters, such as  $T_1$ ,  $T_2$ , and NOE, are often expressed in terms of generalized  $S^2$  order parameters,<sup>2</sup> where  $1 - S^2$  reflects the spatial motional variance of the lattice functions of the relaxation-active interactions.<sup>3</sup> A connection between changes of order parameters and changes of entropy has originally been proposed based on analytical relationships between these quantities for theoretical motional models that describe the motion of backbone N–H atom pairs relative to the rest of the protein.<sup>4</sup> Yang and Kay extended the work to additional motional models including local N–H orientational distributions taken from a molecular dynamics (MD) trajectory.<sup>5</sup> Li, Raychaudhuri, and Wand have proposed a one-dimensional quantum-mechanical vibrator model to translate  $S^2$  changes into entropy changes.<sup>6</sup> Such a translation was also derived for the 3D GAF model.<sup>7</sup> These initial reports have spurred numerous investigations where order parameter changes in polypeptides were linked to thermodynamic quantities from which biologically valuable insight could be gained.<sup>8–20</sup>

A limitation of entropy estimates using this approach is the neglecting of internal motional correlation effects for the atoms

for which experimental order parameters are available.<sup>4</sup> Globular proteins possess a densely packed interior and atomic motions are therefore invariably correlated. Motional correlations can sensitively affect the statistical mechanical partition function and associated thermodynamic quantities. In addition, the number of spins for which relaxation parameters can be extracted is often restricted, thus motional information is available for a protein subsystem only. In Appendix A it is analytically shown for a model system how the partition function of a subsystem becomes less meaningful if its motion is correlated to other degrees of freedom. In many applications, entropy differences rather than absolute entropies are of interest and it is less clear how these are affected by correlated dynamics.

An important practical reason for neglecting correlation effects for data interpretation is the difficulty to derive such information directly from experiment. Detailed information on correlation effects is currently best derived from realistic theoretical models that are molecular-force field based, such as molecular dynamics (MD) computer simulations.<sup>21</sup> An elegant method for the extraction of important aspects of correlated motions from MD trajectories is based on quasiharmonic analysis,<sup>22,23</sup> also known as principal component analysis and essential dynamics.<sup>24</sup> Over recent years, quasiharmonic analysis has become widely recognized as a powerful tool to characterize large-amplitude protein motion along low-dimensional subspaces.<sup>25–29</sup> Quasiharmonic analysis is based on the diagonalization of the covariance matrix of the atomic positions extracted from a structural ensemble, which is typically derived from a MD trajectory. From the eigenvalues of the covariance matrix the conformational partition function can be evaluated from which thermodynamic quantities such as the free energy and the entropy can be directly determined.<sup>22</sup> LeMaster has used quasiharmonic analysis in torsion-angle space to describe correlated dynamics between side chains and the protein backbone.<sup>14</sup> In a recent study by Wrabl, Shortle, and Woolf, entropy changes were estimated from changes of backbone N–H vector fluctuations and were compared with the total entropy change using quasiharmonic analyses for the native and denatured states of staphylococcal nuclease.<sup>30</sup>

Most quasiharmonic modes have both a translational and a reorientational character, i.e., the relative intramolecular motion

\* Correspondence to be addressed to: Prof. Rafael Brüschweiler. Gustaf H. Carlson Chair. Carlson School of Chemistry and Biochemistry, Clark University, Worcester, MA 01610-1477. Phone: (508) 793-7220. Fax: (508) 793-8861. E-Mail: bruschweiler@nmr.clarku.edu.

of two protein fragments may involve both translation and reorientation. Since heteronuclear spin relaxation is solely determined by reorientational motion, we have recently developed a collective axial fluctuation (CAF) model.<sup>31</sup> It is based on the second moment covariance matrix of purely reorientational, spin-relaxation active motion extracted from a MD trajectory. When applied to a protein it allows one to apprehend and analyze reorientational motional correlation effects between different protein fragments, such as different peptide planes.

Here, we use this approach in a more general form to investigate whether a partition function can be defined that is physically meaningful and that reflects larger scale reorientational motion as manifested in NMR spin relaxation experiments. A MD trajectory of ubiquitin is analyzed in terms of a set of second moment covariance matrices. Backbone motion is divided into spin-relaxation active motions involving reorientational dynamics of N–H and C $\alpha$ –H $\alpha$  pairs and other types of motion only involving heavy atoms. From the covariance matrices probability densities are derived from which effective potential functions are obtained that are quadratic in the molecular coordinates. The corresponding quasiharmonic conformational partition functions can be analytically integrated and expressed in terms of the eigenvalues of the covariance matrices. It is shown that the total partition function can be factorized in good approximation into a reorientational part and a remaining part. In this way, a direct link between the thermodynamic properties derived from the reorientational partition function, that includes correlation effects, and NMR relaxation parameters can be established. Finally, the sensitivity of spin-relaxation based entropy changes to the presence of correlated motion is analyzed.

The remainder of the paper is organized as follows: In Section 2, the statistical mechanical theory of reorientational quasiharmonic dynamics is developed. It is applied in Section 3 to a 1.5 ns MD trajectory of ubiquitin for two different models of backbone dynamics. The Conclusion section, 4, is followed by appendices in which basic properties of motional correlations and quasiharmonic descriptions are analytically illustrated.

## 2. Theory

The theory presented here is concerned with the classical part of the partition function of a protein to address relative changes of thermodynamic parameters between different protein states as probed by heteronuclear spin relaxation experiments. It is well-known that quantum-mechanical zero-point motional effects of high-frequency vibrational modes affect absolute values of thermodynamic quantities<sup>21</sup> and NMR relaxation parameters.<sup>32–34</sup> However, the quite uniform behavior of these effects suggests that they are unimportant for the discussion of changes of thermodynamic and spin relaxation quantities between different states, respectively, and therefore will not be further addressed here.

The classical partition function can be written as the product

$$Z_{\text{class}} = Z_{\text{kin}} \cdot Z_{\text{overall}} \cdot Z_{\text{intra}} \quad (1)$$

where  $Z_{\text{kin}}$  represents the kinetic energy part of the partition function,  $Z_{\text{overall}}$  is the partition function belonging to the six coordinates that specify the center of mass and the overall orientation of the molecule, and  $Z_{\text{intra}}$  is the classical conformational partition function given by the integral over conformations  $|R\rangle$  (denoted in Dirac's bracket notation<sup>35</sup>)

$$Z_{\text{intra}} = c \int_{|R\rangle} e^{-V(|R\rangle)/kT} d|R\rangle \quad (2)$$

where prefactor  $c$  renders  $Z_{\text{intra}}$  unit free, but does not affect changes of thermodynamic quantities derived from  $Z_{\text{intra}}$  (vide infra).  $V(|R\rangle)$  is the potential energy function of the protein in conformation  $|R\rangle$ , where  $|R\rangle = |x_1, y_1, z_1, x_2, y_2, z_2, \dots, x_n, y_n, z_n\rangle$  is a  $3n$ -dimensional vector in Cartesian space describing a conformation of the protein consisting of  $n$  atoms and the integral extends over the conformational space accessible to the protein. Note that  $|R\rangle$  is represented in a molecular frame, i.e., the 6 overall motional degrees of freedom have been removed by reorienting and translating each conformation with respect to a reference frame.

Assuming that the protein dynamics can be adequately described by the quasiharmonic approximation, its potential energy can be expressed as a quadratic function<sup>22</sup>

$$V(|R\rangle) = \frac{kT}{2} \langle \Delta R | \mathbf{K}^{-1} | \Delta R \rangle \quad (3)$$

where  $k$  is Boltzmann's constant.  $V(|R\rangle)$  explicitly depends on the absolute temperature  $T$ , and  $|\Delta R\rangle = |R\rangle - |\bar{R}\rangle$  where  $|\bar{R}\rangle$  is the average structure, indicated by the horizontal bar, over the whole structural ensemble. The latter can originate from a molecular dynamics (MD) simulation, a Monte Carlo (MC) simulation, or NMR structure determination. An estimate for the covariance matrix  $\mathbf{K}$ , whose inverse enters eq 3, is obtained from the structural ensemble

$$\mathbf{K} = \overline{|\Delta R\rangle \langle \Delta R|} = \overline{|R\rangle \langle R|} - \overline{|R\rangle} \overline{\langle R|} \quad (4)$$

It immediately follows that  $\mathbf{K}$  becomes singular, i.e., one or more eigenvalues are zero, if the number of structures of the ensemble is smaller than  $3n$ . Insertion of eqs 3, 4 into eq 2 yields  $Z_{\text{intra}}$  reflecting all, i.e., both translational and reorientational, intramolecular motions. The integral for  $Z_{\text{intra}}$  of eq 2 can be analytically determined by transformation into the (orthonormal) eigenbasis  $\{|m\rangle\}$  of matrix  $\mathbf{K}$ ,  $\mathbf{K}|m\rangle = \lambda_m|m\rangle$ , and by expanding  $|\Delta R\rangle$  in this basis,  $|\Delta R\rangle = \sum_m a_m|m\rangle$  with coefficients  $a_m = \langle m|\Delta R\rangle$ . Insertion into eq 3 yields

$$V(|\Delta R\rangle) = \frac{kT}{2} \sum_m \frac{\langle m|\Delta R\rangle^2}{\lambda_m} \quad (5)$$

which reflects that the energetic cost for an excursion along mode  $|m\rangle$  is proportional to the inverse of the eigenvalue  $\lambda_m$ . It follows

$$Z_{\text{intra}} = c \prod_{m=1}^q \int_{|R\rangle} d|R\rangle e^{-\langle m|\Delta R\rangle^2/(2\lambda_m)} = c \prod_{m=1}^q (2\pi\lambda_m)^{1/2} \quad (6)$$

where  $q$  is the total number of quasiharmonic modes. Using standard statistical mechanics methods<sup>36</sup> expressions can be obtained for the Helmholtz free energy

$$A_{\text{intra}} = \bar{V} - TS_{\text{intra}} = -kT \ln Z_{\text{intra}} \quad (7)$$

and for the entropy

$$S_{\text{intra}} = \bar{V}/T + k \ln Z_{\text{intra}} \quad (8)$$

The conformational average of the potential energy,  $\bar{V}$ , can also be evaluated analytically using Gaussian integration leading to the well-known equipartition principle for the harmonic

oscillator stating that each mode has an average potential energy equal to the average kinetic energy  $kT/2$ .<sup>36</sup> Thus,

$$S_{\text{intra}} = \frac{1}{2}kq + k \ln c + \frac{1}{2}kq \ln(2\pi) + \frac{1}{2}k \sum_m \ln \lambda_m \quad (9)$$

which corresponds to eq 10 of Karplus and Kushick.<sup>22</sup>

We now show how the potential function  $V(|\Delta R\rangle)$  can be approximated as a sum of two terms that act on separate coordinate subspaces. The first term is caused by reorientational motions that are spin-relaxation active and the second term is due to all other motion. To illustrate the concept, we divide the whole protein, or the part of it we are interested in, into  $N$  internally rigid fragments, such as the peptide bonds along the protein backbone. The position of the nitrogen atom of peptide plane  $k$  is represented by the vector  $|r_{k0}\rangle = |x_k, y_k, z_k\rangle$  and the orientation of the peptide plane is defined by three ‘auxiliary’ atoms located at

$$|r_{k1}\rangle = |r_{k0}\rangle + |e_{k1}\rangle, |r_{k2}\rangle = |r_{k0}\rangle + |e_{k2}\rangle, |r_{k3}\rangle = |r_{k0}\rangle + |e_{k3}\rangle \quad (10)$$

where  $|e_{k1}\rangle, |e_{k2}\rangle, |e_{k3}\rangle$  are three-dimensional orthogonal vectors of, for example, 1 Å length. Thus, the total number of atoms is  $n = 4N$ . Since this model captures the fully anisotropic motions of the peptide planes, it is particularly well-suited for the combined interpretation of backbone  $^{15}\text{N}$  and  $^{13}\text{C}$  spin relaxation.<sup>31,37,38</sup>

Under certain conditions the covariance matrix  $\mathbf{K}$  adopts a form

$$\mathbf{K} \equiv \begin{pmatrix} \mathbf{K}' & \\ & \mathbf{M} \end{pmatrix} \quad (11)$$

consisting of a part  $\mathbf{M}$  that is exclusively determined by reorientational motion of the peptide planes and a part  $\mathbf{K}'$  that includes remaining heavy atom motion. Sufficient conditions for eq 11 are the following:

1. For the position vectors  $|r_{k1}\rangle, |r_{k2}\rangle, |r_{k3}\rangle$  given in eq 10,  $|r_{k0}\rangle$  can be replaced by its ensemble average  $|r_{k0}\rangle$ .
2. The covariances between vectors  $|r_{k0}\rangle$  and  $|r_{lm}\rangle$  ( $m = 1, 2, 3$ ) vanish.

Matrices  $\mathbf{K}'$  and  $\mathbf{M}$  can then be expressed as

$$\mathbf{K}' = \overline{|\Delta R_0\rangle\langle\Delta R_0|} \quad (12)$$

with the  $3N$ -dimensional vectors  $|\Delta R_0\rangle = ||r_{10}\rangle, \dots, |r_{N0}\rangle\rangle - ||r_{10}\rangle, \dots, |r_{N0}\rangle\rangle$  and

$$\mathbf{M} = \overline{|\Delta e\rangle\langle\Delta e|} \quad (13)$$

depending on the  $9N$ -dimensional vectors

$$|\Delta e\rangle = ||e_{11}\rangle, |e_{12}\rangle, |e_{13}\rangle, \dots, |e_{N1}\rangle, |e_{N2}\rangle, |e_{N3}\rangle\rangle - \overline{||e_{11}\rangle, |e_{12}\rangle, |e_{13}\rangle, \dots, |e_{N1}\rangle, |e_{N2}\rangle, |e_{N3}\rangle\rangle} \quad (14)$$

where the elements of the vectors  $|\Delta R_0\rangle$  and  $|\Delta e\rangle$  have been suitably sorted. The  $9N \times 9N$  matrix  $\mathbf{M}$  is an extension of the recently proposed collective axial fluctuation (CAF) model.<sup>31</sup> This model, which is a generalization of the 3D GAF model,<sup>7,38</sup> employs a  $3N \times 3N$  matrix with elements defined by the scalar product  $\overline{\langle\Delta e_{ik}|\Delta e_{jl}\rangle}$  that are related to matrix  $\mathbf{M}$  of eq 13

by trace formation over  $3 \times 3$  submatrices  $\overline{|\Delta e_{ik}\rangle\langle\Delta e_{jl}|}$ , i.e.,  $\langle\Delta e_{ik}|\Delta e_{jl}\rangle = \text{Tr}\{\overline{|\Delta e_{ik}\rangle\langle\Delta e_{jl}|}\}$ .

The potential energy for a given snapshot can then be decomposed into a part  $V_{\text{active}}$  that belongs to  $\mathbf{M}$  representing spin-relaxation active motion and a part  $V_{\text{other}}$  that belongs to  $\mathbf{K}'$  representing all other (relaxation-inactive) motions:

$$V = V_{\text{active}} + V_{\text{other}} \quad (15)$$

$$V_{\text{active}}(|\Delta e\rangle) = \frac{kT}{2} \langle\Delta e|\mathbf{M}^{-1}|\Delta e\rangle \quad (16)$$

$$V_{\text{other}}(|\Delta R_0\rangle) = \frac{kT}{2} \langle\Delta R_0|\mathbf{K}'^{-1}|\Delta R_0\rangle \quad (17)$$

Since  $V_{\text{active}}(|\Delta e\rangle)$  and  $V_{\text{other}}(|\Delta R_0\rangle)$  act on separate coordinate subspaces, separate partition functions,  $Z_{\text{active}}$  and  $Z_{\text{other}}$ , can be defined using equations analogous to eqs 2, 5, 6, with their product equal to

$$Z_{\text{intra}} = Z_{\text{active}} \cdot Z_{\text{other}} \quad (18)$$

Thus, thermodynamic quantities, directly related to spin-relaxation active motions, can be derived from  $Z_{\text{active}}$ . Since thermodynamic quantities derived from  $Z_{\text{active}}$  reflect pure reorientational motions, we term these quantities ‘reorientational free energy’, ‘reorientational entropy’, etc. The validity of eq 15 will be tested using a MD simulation in the following section.

Changes of conformational entropy between two different states I and II of a protein, such as a bound and a free state, solely depend on the eigenvalues of the matrices  $\mathbf{K}$ ,  $\mathbf{K}'$ , and  $\mathbf{M}$ :

$$\Delta S_{\text{II,I}} = S_{\text{II}} - S_{\text{I}} = \frac{1}{2}k \sum_m \ln(\lambda_{\text{II},m}/\lambda_{\text{I},m}) \cong \Delta S_{\text{active}} + \Delta S_{\text{other}} \quad (19)$$

$$\Delta S_{\text{active}} = S_{\text{active,II}} - S_{\text{active,I}} = \frac{1}{2}k \sum_m \ln(\lambda'_{\text{II},m}/\lambda'_{\text{I},m}) \quad (20)$$

$$\Delta S_{\text{other}} = S_{\text{other,II}} - S_{\text{other,I}} = \frac{1}{2}k \sum_m \ln(\lambda''_{\text{II},m}/\lambda''_{\text{I},m}) \quad (21)$$

where  $\lambda$ ,  $\lambda'$ ,  $\lambda''$  denote the eigenvalues of  $\mathbf{K}$ ,  $\mathbf{M}$ , and  $\mathbf{K}'$ , respectively. Equation 20 yields the change of entropy reflected in changes of local reorientational motion as observable by NMR relaxation spectroscopy.

**Mode Selection Criteria.** So far, we have not mentioned whether all modes or only a subset of modes should be included in eqs 5, 6, 16, 17, 19–21. Obviously, in the presence of constraints (fixed bond lengths, fixed bond angles, etc.) the number of degrees of freedom and thus the number of independent modes is reduced. The protein backbone model described above contains  $4N$  atoms (eq 10). For each of the  $N$  amino acids 3 bond lengths and 3 bond angles are kept fixed. Thus, the total number of degrees of freedom is  $3 \cdot 4N - 6N = 6N$ . For the reorientational covariance matrix  $\mathbf{M}$  the number of degrees of freedom is reduced accordingly from  $9N$  to  $3N$ , while matrix  $\mathbf{K}'$  retains the dimension  $3N$ . One might expect that both matrices  $\mathbf{K}$  and  $\mathbf{M}$  determined from a MD simulation using eqs 4 and 13 are singular, each with  $6N$  eigenvalues equal to zero. However,  $\mathbf{K}$  and  $\mathbf{M}$  are generally found to be nonsingular due to the neglecting of higher order ( $>2$ ) correlations present in

the original MD simulation. The situation is analytically illustrated in Appendix B at the example of a quasiharmonic analysis of a system with one degree of freedom consisting of two orthogonal vectors exhibiting Gaussian reorientational motion about an orthogonal axis. As a consequence, for  $\mathbf{K}$  only the dominant  $6N$  modes (i.e., the  $6N$  modes with largest eigenvalues) and for  $\mathbf{M}$  the dominant  $3N$  modes should be included for the evaluation of energies and entropies as will be described in the following section.

### 3. Application

**MD Computer Simulation of Ubiquitin.** The theory described in the previous section was applied to 1500 snapshots of the 76 amino acid protein ubiquitin from a 1.5 ns MD trajectory stored with a time increment of 1 ps. An all-atom representation of the protein was embedded in a cubic box including 2909 explicit water molecules, and the simulation was carried out using the program CHARMM 24<sup>39,40</sup> under periodic boundary conditions and at a temperature of 300 K. More details on the simulation can be found in ref 38. Before the covariance matrices were calculated, the overall translational and reorientational motion was removed by optimally superimposing the atoms of each snapshot on the ones of the snapshot at 750 ps. Quasiharmonic and reorientational quasiharmonic analyses were carried out on backbone atoms with coordinates taken from the trajectory as described below. While side-chain atoms are not explicitly taken into account in these analyses, their presence in the MD force field used to generate the trajectory implicitly affect the motions and covariance properties of the backbone atoms.

**Idealized Peptide Plane Dynamics.** A quasiharmonic analysis was performed on the 72 nonproline peptide bonds along the main chain yielding matrix  $\mathbf{K}$ . Each peptide bond is represented by its nitrogen atom together with three auxiliary atoms, that probe local reorientational motion of the peptide planes, leading to a total of  $4N$  atoms. The three auxiliary atoms are positioned along three orthogonal directions from the nitrogen atom at a distance of 1 Å. The first auxiliary atom is placed parallel to the  $\mathbf{C}_{i-1}^\alpha - \mathbf{C}_i^\alpha$  direction, the second atom is in the peptide plane orthogonal to the  $\mathbf{C}_{i-1}^\alpha - \mathbf{C}_i^\alpha$  axis, and the third atom is placed orthogonal to the peptide plane. This leads to  $3 \cdot 4N = 864$  Cartesian coordinates and the same number of quasiharmonic modes from which only the  $6N = 432$  modes with largest amplitude were considered for the energy function  $V$  of eq 5 (see discussion of the previous section). For  $\mathbf{K}'$  a reduced quasiharmonic analysis was performed on the 72 nitrogen atoms only, leading to  $3N = 216$  quasiharmonic modes, all of which were included in the evaluation of the energy function  $V_{\text{other}}$  (eq 17). For matrix  $\mathbf{M}$  a  $9N = 648$  dimensional reorientational quasiharmonic analysis was performed by following eqs 13 and 16, from which the smallest  $6N$  modes were excluded from the evaluation of  $V_{\text{active}}$ .

For each of the 1500 snapshots  $V$ ,  $V_{\text{active}}$ ,  $V_{\text{other}}$  were calculated in order to examine the validity of the relationship  $V = V_{\text{active}} + V_{\text{other}}$ . A plot of  $V_{\text{active}} + V_{\text{other}}$  vs  $V$  is shown in Figure 1a. Linear regression yields a slope of 1.003 and a correlation coefficient of 0.89. The relaxation-active motions are thus in good approximation separable from other motions and the relaxation-active partition function  $Z_{\text{active}}$  is a well-defined quantity for this model of protein backbone dynamics. The relaxation-active motions are clearly less correlated with respect to remaining motions as is seen in Figure 1b, where  $V_{\text{other}}$  is plotted vs  $V_{\text{active}}$ , exhibiting a correlation coefficient of 0.64.

**Protein Backbone Dynamics Model for  $\text{C}^\alpha\text{--H}^\alpha$  and  $\text{N--H}^\text{N}$  spin relaxation.** A more realistic model for protein backbone

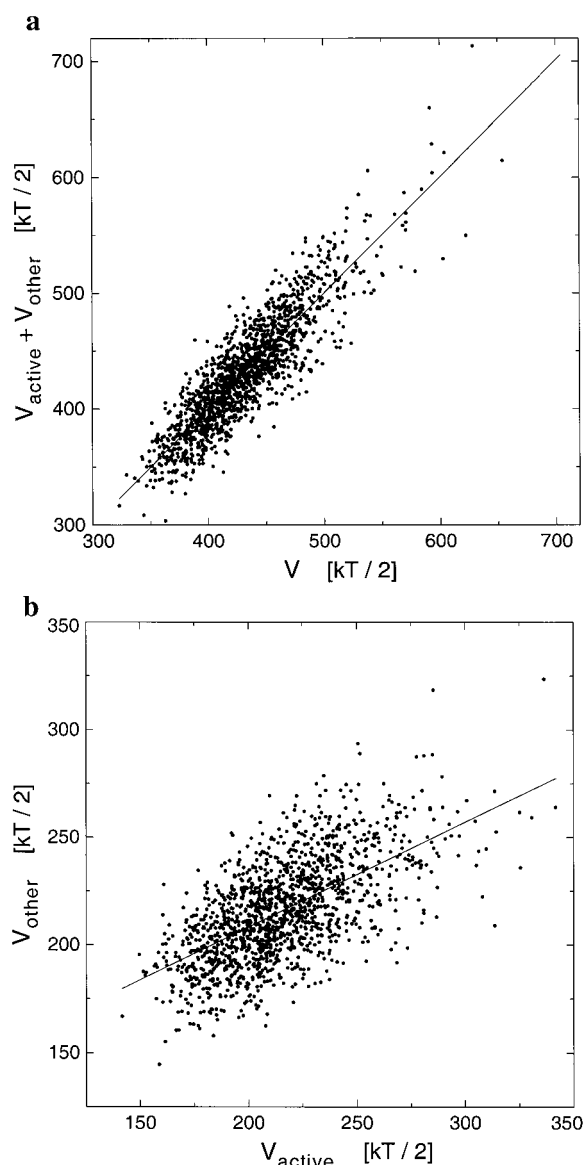


**Figure 1.** Correlation of (a)  $V_{\text{active}} + V_{\text{other}}$  vs  $V$  and (b)  $V_{\text{other}}$  vs  $V_{\text{active}}$  for the idealized backbone model in the quasiharmonic approximation for 1500 snapshots of ubiquitin using eqs 5, 16, and 17. The calculations include the largest  $6N$  quasiharmonic modes for  $V$ , and the largest  $3N$  modes for  $V_{\text{other}}$  and  $V_{\text{active}}$ , where  $N = 72$  is the number of included (nonproline) residues. All energies are given in units of  $kT/2 = 1.247$  kJ·mol<sup>-1</sup> (at  $T = 300$  K). In panel (a) 1 point and in panel (b) 5 points fall outside the plotted region.

dynamics that explicitly includes the internuclear vectors  $\text{N--H}^\text{N}$  and  $\text{C}^\alpha\text{--H}^\alpha$  that determine  $^{15}\text{N}$  and  $^{13}\text{C}^\alpha$  spin relaxation via magnetic dipolar interactions consists of the backbone  $\text{N}$ ,  $\text{H}^\text{N}$ ,  $\text{C}^\alpha$ ,  $\text{H}^\alpha$  atoms of the nonproline residues. We refer to this model as the NHCH model. A quasiharmonic, a reduced quasiharmonic, and a reorientational quasiharmonic analysis were performed: matrix  $\mathbf{K}$  was determined based on (nonproline)  $\text{N}$ ,  $\text{H}^\text{N}$ ,  $\text{C}^\alpha$ ,  $\text{H}^\alpha$  atoms, matrix  $\mathbf{K}'$  based on (nonproline)  $\text{N}$  and  $\text{C}^\alpha$  atoms, and matrix  $\mathbf{M}$  was determined based on the internuclear vectors  $\text{N--H}^\text{N}$  and (nonproline)  $\text{C}^\alpha\text{--H}^\alpha$ . The bond lengths of  $\text{N--H}^\text{N}$  and  $\text{C}^\alpha\text{--H}^\alpha$  were kept fixed at 0.997 and 1.083 Å, respectively, but bending motions were not artificially constrained. The dimension of  $\mathbf{K}$  is  $4 \cdot 3N = 864$  while  $\mathbf{K}'$  and  $\mathbf{M}$  have the same dimension  $2 \cdot 3N = 432$ . The eigenvalues  $\lambda$  of matrices  $\mathbf{K}$ ,  $\mathbf{K}'$ , and  $\mathbf{M}$  are given in Figure 2 together with the corresponding mode collectivities  $\kappa^{41}$  defined in Appendix C. Large eigenvalues  $\lambda$  correspond to large amplitude modes. The



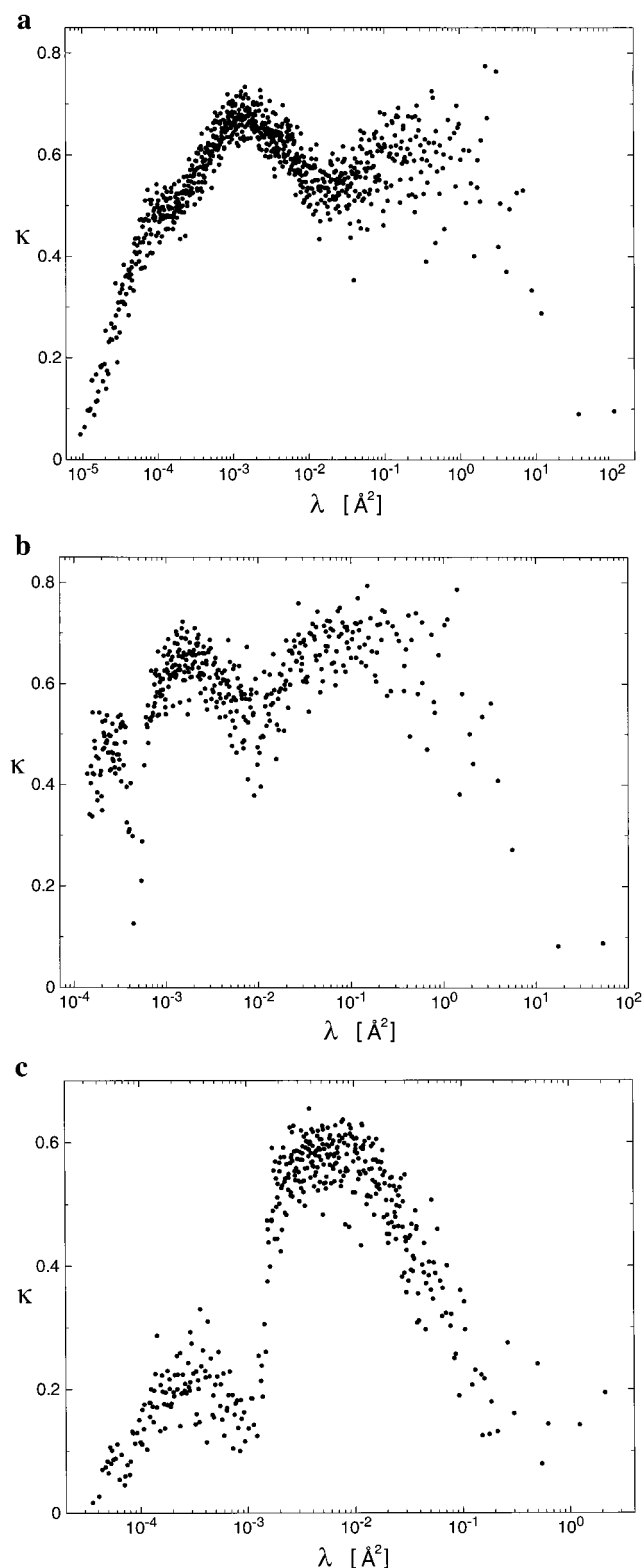


**Figure 2.** Mode collectivities  $\kappa$  vs eigenvalues  $\lambda$  of covariance matrices (a)  $\mathbf{K}$ , (b)  $\mathbf{K}'$ , and (c)  $\mathbf{M}$  (eqs 4, 12, 13) for the NHCH protein backbone model of ubiquitin.  $\kappa$ , which varies between zero and one, is a measure for the effective number atoms or internuclear vectors that are significantly affected by a certain mode: in case of  $\mathbf{K}$  these are the N,  $\text{H}^{\text{N}}$ ,  $\text{C}^{\alpha}$ ,  $\text{H}^{\alpha}$  atoms, in case of  $\mathbf{K}'$  these are the N and  $\text{C}^{\alpha}$  atoms, and in case of  $\mathbf{M}$  these are the N–H and  $\text{C}^{\alpha}$ – $\text{H}^{\alpha}$  vectors.

collectivity  $\kappa$  denotes the relative number of atoms (or internuclear vectors in the case of  $\mathbf{M}$ ) that are significantly affected by a certain mode.  $\kappa$  is a scalar function of an eigenmode independent of the eigenvalue and it can take values between

$1/n_{\text{max}}$  and 1, where  $n_{\text{max}}$  is the total number of fragments: if a mode uniformly affects all fragments then  $\kappa = 1$ , and if only one fragment is affected then  $\kappa = 1/n_{\text{max}}$ . For some of the small-amplitude backbone modes, reorientational and other types of motion are not separable. Since the effect of these modes on spin relaxation data is uniform and small,<sup>32,42,43</sup> they can be included in a separate partition function, possibly of a quantum-mechanical nature,<sup>36</sup> which does hardly reflect changes of NMR relaxation data.

The eigenvalues of matrices  $\mathbf{K}$ ,  $\mathbf{K}'$ , and  $\mathbf{M}$  range over 7, 6, and 5 orders of magnitude, respectively. As explained above, none of the eigenvalues are zero and there is also no clear gap between soft and (partially) constrained degrees and freedom. The collectivities  $\kappa$  are generally lowest for the smallest and the largest amplitude modes with local minima in between. For  $\mathbf{K}$ ,  $\mathbf{K}'$ , and  $\mathbf{M}$  the collectivity  $\kappa$  is for all modes below 0.77, 0.79, and 0.65, respectively. For  $\mathbf{K}$  there are about  $3N = 216$  modes with eigenvalues larger than the pronounced minimum in the center and  $9N = 648$  modes with eigenvalues that are smaller. For  $\mathbf{K}'$  (panel b), the group of modes at the low-amplitude end contains  $N = 72$  modes presumably caused by the restricted N– $\text{C}^{\alpha}$  bond lengths. Even for low-amplitude modes the collectivities are on average rather high, unlike the small collectivities found in the high-frequency spectrum of a normal-mode analysis of crambin.<sup>41</sup> The collectivities of the reorientational modes (panel c) are lower than the quasiharmonic modes, particularly in the high-amplitude and the low-amplitude regimes. The low-amplitude regime, which includes  $1.75N = 126$  modes, is separated from the rest by a sharp drop in collectivity. By comparing the collectivities between Figure 2a and Figure 2b,c it can be seen that eq 11 is an approximation.

As was already noted for the idealized peptide-plane dynamics model, some small-amplitude modes are nonphysical and others are nonseparable in the sense of eq 15. Since these modes have little influence on changes in NMR relaxation parameters, only larger amplitude modes are included in the following discussion. The two constraints imposed on the N– $\text{H}^{\text{N}}$  and  $\text{C}^{\alpha}$ – $\text{H}^{\alpha}$  bond lengths lead to a formal reduction of the actual number of degrees of freedom of  $\mathbf{K}$  and  $\mathbf{M}$  by  $2N$ . Potential energies  $V$ ,  $V_{\text{active}}$ , and  $V_{\text{other}}$  were calculated using eqs 5, 16, and 17 with the smallest  $2N$  modes excluded from  $V$  and  $V_{\text{active}}$ .  $V_{\text{active}} + V_{\text{other}}$  vs  $V$  is plotted in Figure 3a. The correlation coefficient of 0.82 and the slope of 1.12 are quite similar to the results of Figure 1a. From the relationship  $V \cong V_{\text{active}} + V_{\text{other}}$  follows that the conformational partition function can in good approximation be partitioned into a relaxation-active reorientational part and a remaining part. As in Figure 1b,  $V_{\text{active}}$  and  $V_{\text{other}}$  exhibit a substantially lower correlation with a correlation coefficient of 0.46.

The number of modes can be further reduced if degrees of freedom associated with the two bond angles  $\text{H}^{\text{N}}$ –N– $\text{C}^{\alpha}$  and N– $\text{C}^{\alpha}$ – $\text{H}^{\alpha}$  and the bond length N– $\text{C}^{\alpha}$  are excluded. Thus, the number of degrees of freedom for  $\mathbf{K}$  is  $12N - 5N = 7N$ , for  $\mathbf{K}'$   $6N - N = 5N$ , and for  $\mathbf{M}$   $6N - 4N = 2N$ . Potential energies computed from the remaining largest modes are shown in Figure 3b. The correlation coefficient between  $V_{\text{active}} + V_{\text{other}}$  and  $V$  is 0.84 with a slope of 1.05, while the correlation coefficient between  $V_{\text{active}}$  and  $V_{\text{other}}$  is 0.51. Although fewer modes are included, the width of the energy distribution is hardly affected as compared to Figure 3a. It is instructive to analyze also energies  $V'$ ,  $V'_{\text{active}}$ , and  $V'_{\text{other}}$  associated with the small-amplitude modes that were excluded in Figure 3b. These are  $5N$  modes in  $\mathbf{K}$ ,  $N$  modes for  $\mathbf{K}'$ , and  $4N$  modes for  $\mathbf{M}$ .

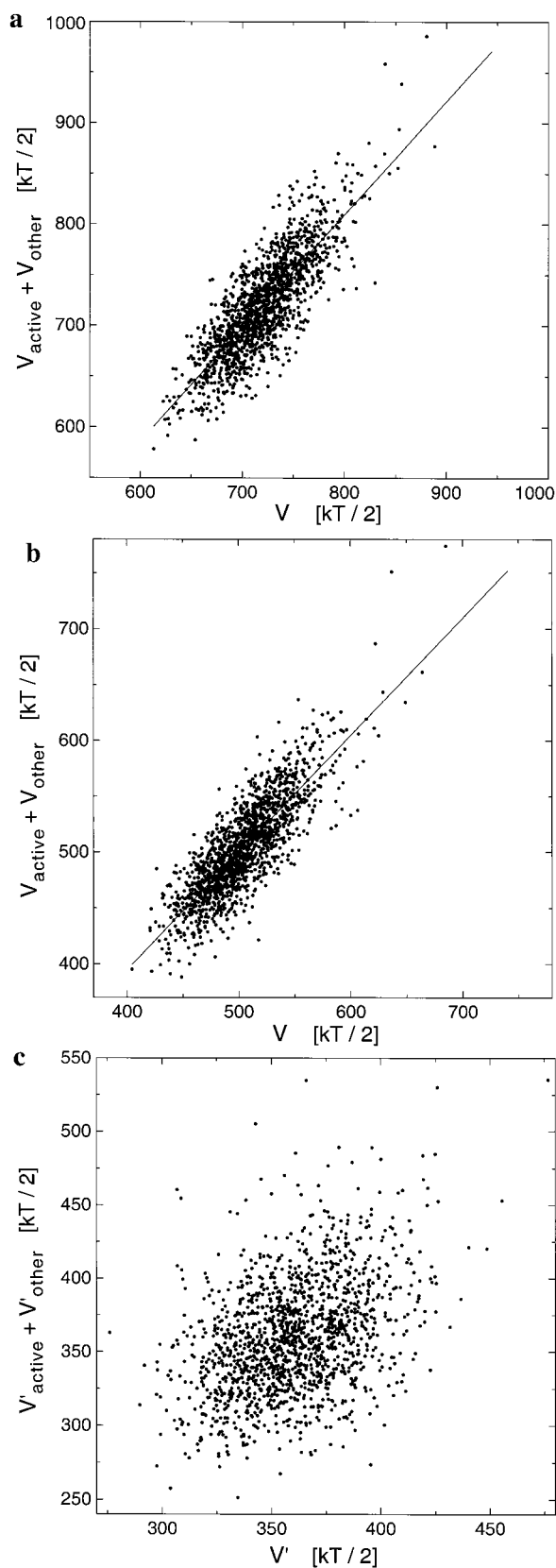


**Figure 3.** Correlation of  $V_{\text{active}} + V_{\text{other}}$  vs  $V$  for the NHCH backbone model of ubiquitin with  $N = 72$  peptide planes. In panel (a) the largest  $6N$ ,  $4N$ , and  $10N$  modes and in panel (b) the  $5N$ ,  $2N$ , and  $7N$  modes with largest amplitude have been included for the calculation of  $V_{\text{other}}$ ,  $V_{\text{active}}$ , and  $V$ , respectively. In panel (c) the  $N$ ,  $4N$ , and  $5N$  modes with smallest amplitude have been included for  $V_{\text{other}}$ ,  $V_{\text{active}}$ , and  $V$ , respectively. All energies are given in units of  $kT/2 = 1.247 \text{ kJ} \cdot \text{mol}^{-1}$  (at  $T = 300 \text{ K}$ ). In panels (a) and (b) one point falls outside the plotted region.

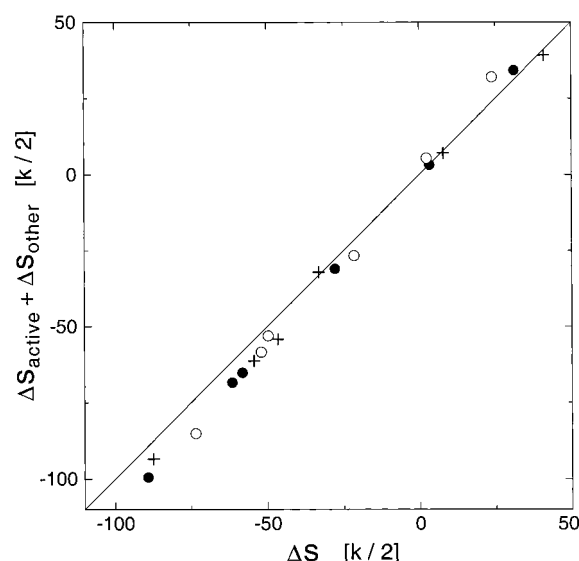


**Figure 4.** Entropy differences  $\Delta S_{\text{active}} + \Delta S_{\text{other}}$  vs  $\Delta S$  between the four ubiquitin parts 1–4, each including 18 amino acids, calculated using eqs 19–21. The “+” symbols refer to the idealized peptide-plane model, the “●” symbols to the NHCH model of Figure 3a and the “○” symbols to the NHCH model of Figure 3b. The entropy differences are given in units of  $k/2 = 4.157 \text{ J} \cdot \text{mol}^{-1} \cdot \text{K}^{-1}$ .

$V_{\text{active}} + V_{\text{other}}$  vs  $V'$  is plotted in Figure 3c. The low correlation between the energy terms (correlation coefficient of 0.40) indicates that for these modes relaxation-active components are not separable from remaining ones. While this is inconsequential for nuclear spin relaxation data interpretation, it may be relevant for the thermodynamic interpretation of dynamics data obtained by other spectroscopic techniques that can resolve higher frequency motions, such as multidimensional infrared spectroscopy.<sup>44</sup>

The existence of the relationship  $V \cong V_{\text{active}} + V_{\text{other}}$ , supported by Figures 1, 3, implies separability of the partition function into a product  $Z_{\text{intra}} \cong Z_{\text{active}} \cdot Z_{\text{other}}$  (eq 18). The validity of this relationship is further explored by calculating entropy differences using the relationship  $\Delta S \cong \Delta S_{\text{active}} + \Delta S_{\text{other}}$  (see eqs 19–21) for two protein states. For this purpose ubiquitin was divided into four parts, each representing the backbone atoms of 18 sequential (nonproline) amino acids. Part 1 contains the N-terminal  $\beta$ -sheet, part 2 contains the central  $\alpha$ -helix, part 3 includes two  $\beta$ -strands, and part 4 includes one  $\beta$ -strand and the C-terminal end. A figure with collectivities and eigenvalues of the  $M$  matrices for the NHCH model of the 4 parts of ubiquitin is provided as Supporting Information. Each part exhibits characteristic dynamics behavior as has been described previously<sup>31,38</sup> in qualitative agreement with experiment.<sup>38,45,46</sup> For each of the four parts the entropies  $S$ ,  $S_{\text{active}}$ , and  $S_{\text{other}}$  were calculated and pairwise differences were determined. The analysis was carried out for the idealized peptide-plane dynamics model with  $6N$  modes and for the NHCH model with  $10N$  and  $7N$  modes, respectively. The results are shown in Figure 4, where  $\Delta S_{\text{active}} + \Delta S_{\text{other}}$  vs  $\Delta S$  is plotted for 6 pairwise differences of the four protein parts. The high degree of linearity of the relationship (correlation coefficients  $\geq 0.998$ ), together with slopes that are close to one (1.05, 1.11, and 1.18, respectively) corroborate the above findings that the two types of protein motions sampled on the ns and sub-ns time scales are in good approximation separable in a statistical mechanical sense. The independence of reorientations and other types of motions, including translations, found here is reminiscent of the independence of angular and radial fluctuations of dipolar

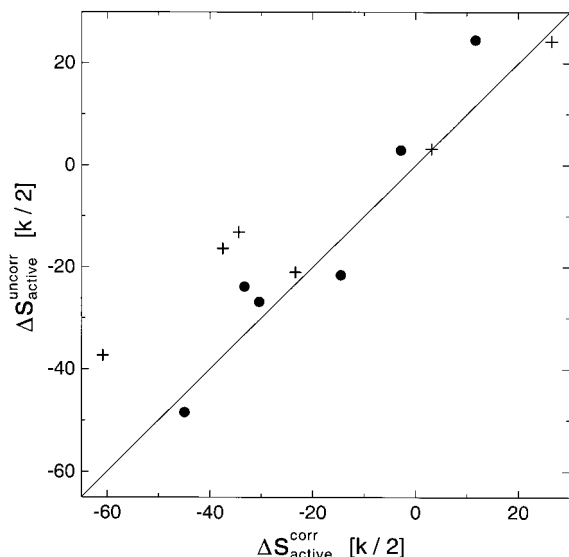


**Figure 5.** Reorientational entropy differences determined in the presence of correlation effects,  $\Delta S_{\text{active}}^{\text{corr}}$ , compared to estimates of entropy differences ignoring correlation effects,  $\Delta S_{\text{active}}^{\text{uncorr}}$ , for the four parts 1–4 of ubiquitin. The same symbols are used for the polypeptide backbone models as in Figure 4. The three “+” symbols furthest away from the diagonal correspond to entropy differences involving part 4. The entropy differences are given in units of  $k/2 = 4.157 \text{ J} \cdot \text{mol}^{-1} \cdot \text{K}^{-1}$ .

interactions previously observed in the context of homonuclear NMR cross relaxation analysis of polypeptides.<sup>47</sup>

#### Effect of Correlation on Reorientational Entropy Changes.

On the basis of the above results, it is possible to quantify the effect of motional correlations on estimates of reorientational entropy differences,  $\Delta S_{\text{reor}}$ , between different protein states. For this purpose, the reorientational entropies are calculated for each of the four protein segments in two different ways: once including correlation and once without correlation. Correlation effects are excluded by modifying the covariance matrix  $\mathbf{M}$  to  $\mathbf{M}'$  by setting certain elements to zero. For the idealized peptide-plane dynamics model these are all elements that connect different peptide planes, while for the NHCH model with  $4N$  modes these are all elements between individual  $\text{N}-\text{H}^{\text{N}}$  and  $\text{C}^{\alpha}-\text{H}^{\alpha}$  vectors, i.e., each dipolar vector is assumed to move in an uncorrelated way from all other dipolar vectors.  $\mathbf{M}'$  is then block-diagonal with each block belonging to a peptide plane or a dipolar vector, respectively. While information about correlations has become lost,  $\mathbf{M}'$  still reflects local spin-relaxation active motions with unchanged amplitudes. Pairwise differences of reorientational entropies can be evaluated using eq 20 in the presence and in the absence of correlation:

$$\Delta S_{\text{reor},ij}^{\text{corr}} = S_{\text{reor},j}^{\text{corr}} - S_{\text{reor},i}^{\text{corr}} \quad \Delta S_{\text{reor},ij}^{\text{uncorr}} = S_{\text{reor},j}^{\text{uncorr}} - S_{\text{reor},i}^{\text{uncorr}} \quad (22)$$

where  $i, j = 1, \dots, 4$  denote the four protein parts whose entropies are compared. In Figure 5  $\Delta S_{\text{reor},ij}^{\text{uncorr}}$  is plotted against  $\Delta S_{\text{reor},ij}^{\text{corr}}$  for all six pairwise reorientational entropy differences between the four parts of ubiquitin for both backbone dynamics models. The degree of correlation is remarkably high with an average correlation coefficient of 0.97 and an average slope of 0.91. This implies that motional correlation effects that are a characteristic feature of the dynamics of ubiquitin have on average a small and in some case a negligible effect on reorientational entropy differences between its different parts. Absolute entropies  $S_{\text{reor},q}^{\text{uncorr}}$  and  $S_{\text{reor},q}^{\text{corr}}$  do significantly differ for fragments 1–3 for the idealized peptide-plane dynamics model

and for all four fragments for the NHCH model with  $4N$  modes with  $S_{\text{reor},q}^{\text{uncorr}}$  clearly larger than  $S_{\text{reor},q}^{\text{corr}}$ . This is consistent with the finding that the neglecting of correlations generally leads to an inflation of the partition function,  $Z_{\text{reor}}^{\text{uncorr}} = \rho Z_{\text{reor}}^{\text{corr}}$ , where  $\rho$  is a scaling factor  $\rho \approx \alpha e^{\beta N}$  with  $\beta$  proportional to the number of included modes and  $\alpha$  as a prefactor. An exception to this behavior is seen for part 4 for the idealized peptide-plane dynamics model, where the high mobility of the C-terminal two peptide planes leads to  $S_{\text{reor},4}^{\text{uncorr}} \approx S_{\text{reor},4}^{\text{corr}}$ . This behavior is not seen for the NHCH model where reorientational motion is probed about different axes.

These findings have the direct consequence that for the system studied here reorientational entropy changes can be estimated with good confidence from local reorientational fluctuations, as monitored by nuclear spin relaxation measurements, without taking correlation effects explicitly into account. This result is quite remarkable and may hold also for other globular protein states. It offers an easy and yet realistic estimate of entropy changes in biomolecules based on NMR spin relaxation experiments. It is expected, however, that the exact nature of motional correlations can have a significant effect on estimates of entropy differences when the motional correlation characteristics of the states to be compared become qualitatively different. The validity range of this approximation can be further explored by application of this type of analysis to partially folded and unfolded protein states (work in progress).

#### 4. Conclusion

Thermodynamic interpretation of relaxation data of proteins and other biomolecules offers a complementary view of their dynamic behavior assisting the understanding of biomolecular function. Due to the presence of strong correlation effects in globular proteins the statistical mechanical separation of reorientational motion amenable to heteronuclear spin relaxation from other types of motion is not obvious and has been demonstrated here for ubiquitin by using a MD simulation and various forms of second moment covariance analyses. It has been shown that for dominant protein motions sampled on the ns time scale an intramolecular reorientational partition function and a reorientational entropy can be defined that are physically meaningful. Moreover, the effect of motional correlation on changes of reorientational entropies between different parts of ubiquitin has been found to be remarkably small. These results provide a theoretical basis toward a more quantitative thermodynamic interpretation of NMR spin relaxation data in biomolecules. The presented concepts should be applicable to other biological and nonbiological macromolecular systems as well.

#### Appendix A

The extent to which motions are correlated critically depends on the choice of the coordinate system and on the considered objects, such as individual atoms, atom pairs, peptide groups, dihedral angles, or internuclear vectors. These factors also determine whether for a subsystem a statistical-mechanical partition function and inferred thermodynamic properties can be meaningfully defined. The problem can be exemplified for a system exhibiting two classical degrees of freedom,  $x$  and  $y$ , with a quadratic potential energy function  $V(x, y)$  characterized by the constants  $a, b$  with  $a, b > 0$

$$V(x, y) = \frac{1}{2}(ax^2 + by^2) = \frac{1}{2}\begin{pmatrix} x \\ y \end{pmatrix}^T \begin{pmatrix} a & 0 \\ 0 & b \end{pmatrix} \begin{pmatrix} x \\ y \end{pmatrix} \quad (\text{A1})$$

The conformational partition function is then

$$Z = \int_{-\infty}^{\infty} \int_{-\infty}^{\infty} dx dy e^{-V(x,y)/(kT)} =$$

$$\left( \int_{-\infty}^{\infty} dx e^{-ax^2/(2kT)} \right) \left( \int_{-\infty}^{\infty} dy e^{-by^2/(2kT)} \right) =$$

$$Z_x Z_y = \frac{2\pi kT}{\sqrt{ab}} \quad (\text{A2})$$

Thermal motions along  $x$  and  $y$  are uncorrelated and the exact partition function can be factorized such that thermodynamic quantities inferred from  $Z_x$ , that are only associated with coordinate  $x$ , are in fact meaningful. The analogous statement holds for coordinate  $y$ .

We now describe the problem in a new coordinate system that is rotated by an angle  $\varphi$  with respect to the old one:  $x' = \cos \varphi x - \sin \varphi y$ ,  $y' = \sin \varphi x + \cos \varphi y$ . The potential energy  $V(x', y')$  is then

$$V(x', y') = \frac{1}{2} \begin{pmatrix} x' \\ y' \end{pmatrix}^T \begin{pmatrix} ac^2 + bs^2 & (a-b)cs \\ (a-b)cs & as^2 + bc^2 \end{pmatrix} \begin{pmatrix} x' \\ y' \end{pmatrix} \quad (\text{A3})$$

where  $c = \cos \varphi$ ,  $s = \sin \varphi$ . The motions along  $x'$  and  $y'$  are correlated provided that the off-diagonal elements  $(a-b)cs \neq 0$ . Obviously, the partition function belonging to  $V(x', y')$  must be the same as the one of eq A2.

If, however, correlation effects between  $x'$  and  $y'$  are ignored, i.e., if the off-diagonal elements of eq A3 are set to zero, then the partition function becomes

$$Z^{\text{uncorr}} =$$

$$\left\{ \int_{-\infty}^{\infty} dx' e^{-(ac^2 + bs^2)x'^2/(2kT)} \right\} \left\{ \int_{-\infty}^{\infty} dy' e^{-(as^2 + bc^2)y'^2/(2kT)} \right\} =$$

$$Z_{x'}^{\text{uncorr}} \cdot Z_{y'}^{\text{uncorr}} = \frac{2\pi kT}{\sqrt{(ac^2 + bs^2)(as^2 + bc^2)}} \quad (\text{A4})$$

Comparison with eq A2 shows that neglecting of correlation effects implies  $Z^{\text{uncorr}} \leq Z$ . Thus  $Z^{\text{uncorr}}$  provides a lower bound for  $Z$ . Except for special cases,  $Z$  cannot be reconstructed from the parts  $Z_{x'}^{\text{uncorr}}$ ,  $Z_{y'}^{\text{uncorr}}$  and hence, thermodynamic quantities of the system, such as free energy and entropy, cannot be represented as sums of thermodynamic quantities individually derived from  $Z_{x'}^{\text{uncorr}}$  and  $Z_{y'}^{\text{uncorr}}$ .

## Appendix B

In this appendix, quasiharmonic analysis of two orthogonal vectors,  $\mathbf{e}_x = (\cos \varphi, \sin \varphi)$  and  $\mathbf{e}_y = (-\sin \varphi, \cos \varphi)$ , lying in the  $xy$  plane undergoing one-dimensional Gaussian reorientational motion<sup>3</sup> about an axis perpendicular to the plane is discussed. It is found that motion along different quasiharmonic modes may maintain phase relationships, which is in contrast to assumptions made in normal-mode analysis.

The state of the system is specified by the 4-dimensional vector  $|\mathbf{e}\rangle = |\mathbf{e}_x, \mathbf{e}_y\rangle = |\cos \varphi, \sin \varphi, -\sin \varphi, \cos \varphi\rangle$ . The normalized probability distribution  $p(\varphi)d\varphi$  of the angle  $\varphi$  is a Gaussian distribution centered around  $\varphi = 0$

$$p(\varphi)d\varphi = (2\pi\sigma_\varphi^2)^{-1/2} e^{-\varphi^2/(2\sigma_\varphi^2)} d\varphi \quad (\text{A5})$$

For  $\sigma_\varphi \ll \pi$ , the matrix  $\mathbf{M}$  of eq 13 can be determined analytically using the relationships<sup>3</sup>  $\cos m\varphi = e^{-m^2\sigma_\varphi^2/2}$  and  $\sin m\varphi = 0$  together with the identities  $\cos^2\varphi = (1 + \cos 2\varphi)/2$ ,  $\sin^2\varphi = (1 - \cos 2\varphi)/2$ , and  $\sin\varphi\cos\varphi = (\sin 2\varphi)/2$

$$\mathbf{M} = \overline{|\Delta\mathbf{e}\rangle\langle\Delta\mathbf{e}|} = \begin{bmatrix} A & 0 & 0 & A \\ 0 & B & -B & 0 \\ 0 & -B & B & 0 \\ A & 0 & 0 & A \end{bmatrix} \quad (\text{A6})$$

where  $|\Delta\mathbf{e}\rangle = |\mathbf{e}\rangle - \overline{|\mathbf{e}\rangle}$  and  $A = 1/2(1 + e^{-2\sigma_\varphi^2} - 2e^{-\sigma_\varphi^2})$ ,  $B = 1/2(1 - e^{-2\sigma_\varphi^2})$ . Diagonalization yields four orthogonal eigenvectors  $\mathbf{v}_1 = (1, 0, 0, 1)$ ,  $\mathbf{v}_2 = (1, 0, 0, -1)$ ,  $\mathbf{v}_3 = (0, 1, 1, 0)$ ,  $\mathbf{v}_4 = (0, 1, -1, 0)$  with eigenvalues  $\lambda_1 = 2A$ ,  $\lambda_2 = \lambda_3 = 0$ ,  $\lambda_4 = 2B$ .

Despite the fact that this system has only one degree of freedom,  $\varphi$ , there are two eigenmodes,  $\mathbf{v}_1$  and  $\mathbf{v}_4$ , with nonzero amplitude (eigenvalues). This implies that the two modes have a well-defined phase relationship as can be seen by spanning an original orientation  $|\mathbf{e}_x, \mathbf{e}_y\rangle$  in the  $\mathbf{v}_1, \mathbf{v}_4$  basis

$$|\mathbf{e}\rangle = |\mathbf{e}_x, \mathbf{e}_y\rangle = \cos\varphi \mathbf{v}_1 + \sin\varphi \mathbf{v}_4 \quad (\text{A7})$$

$$|\Delta\mathbf{e}\rangle = |\mathbf{e}\rangle - \overline{|\mathbf{e}\rangle} =$$

$$|\cos\varphi - e^{-\sigma_\varphi^2/2}, \sin\varphi, -\sin\varphi, \cos\varphi - e^{-\sigma_\varphi^2/2}\rangle =$$

$$(\cos\varphi - e^{-\sigma_\varphi^2/2}) \mathbf{v}_1 + \sin\varphi \mathbf{v}_4 \quad (\text{A8})$$

This example demonstrates that quasiharmonic modes can be correlated. Thus, at a given temperature the modes are not independently populated, if the number of included modes exceeds the actual number of degrees of freedom.

## Appendix C

Eigenmodes  $\vec{Q}_j$  of matrices  $\mathbf{K}$ ,  $\mathbf{K}'$ , and  $\mathbf{M}$  can exhibit a variable degree of delocalization or collectivity with respect to the atoms or internuclear vectors involved. A quantitative measure for the collectivity of a mode is its *mode collectivity index* or simply the *mode collectivity*,  $\kappa$ ,<sup>41</sup> which is calculated from the  $P$  vector components  $\vec{q}_{j,k}$  of  $\vec{Q}_j$ ,  $\vec{Q}_j = (\vec{q}_{j,1}, \vec{q}_{j,2}, \dots, \vec{q}_{j,P})$ , describing the displacement of atoms or the reorientation of vectors

$$\kappa_j = \frac{1}{P} \exp\left\{-\sum_{k=1}^P |\vec{q}_{j,k}|^2 \log|\vec{q}_{j,k}|^2\right\} \quad (\text{A9})$$

$\kappa_j$  is a number between  $1/P$  and 1 given by the ratio between the effective number of fragments that are collectively reoriented by the  $j$ th mode and the total number of fragments. A small  $\kappa$  reflects local motion, while a large  $\kappa$  reflects a substantial degree of collectivity. For the NHCH backbone model  $P = 2N$  while for the idealized peptide plane dynamics model  $P = N$ , where  $N$  is the number of included peptide planes.

**Acknowledgment.** J.J.P. is a recipient of a Human Frontier Science Program postdoctoral fellowship. This work was supported by NSF Grant No. MCB-9904875.

**Supporting Information Available:** A figure with collectivities  $\kappa$  and eigenvalues  $\lambda$  of the  $\mathbf{M}$  matrices for the NHCH model of the four fragments of ubiquitin (PDF). This material is available free of charge via Internet at <http://pubs.acs.org>.

## References and Notes

- (1) Kay, L. E. *Nat. Struct. Biol.* **1998**, 5, 513–517.
- (2) Lipari, G.; Szabo, A. *J. Am. Chem. Soc.* **1982**, 104, 4546–4559; Lipari, G.; Szabo, A. *J. Am. Chem. Soc.* **1982**, 104, 4559–4570.



- (3) Brüschweiler, R.; Wright, P. E. *J. Am. Chem. Soc.* **1994**, *116*, 8426–8427.
- (4) Akke, M.; Brüschweiler, R.; Palmer, A. G. *J. Am. Chem. Soc.* **1993**, *115*, 9832–9833.
- (5) Yang, D.; Kay, L. E. *J. Mol. Biol.* **1996**, *263*, 369–382.
- (6) Li, Z. G.; Raychaudhuri, S.; Wand, A. J. *Prot. Sci.* **1996**, *5*, 2647–2650.
- (7) Bremi, T.; Brüschweiler, R. *J. Am. Chem. Soc.* **1997**, *119*, 6672–6673.
- (8) Stivers, J. T.; Abeygunawardana, C.; Mildvan, A. S.; Whitman, C. P. *Biochemistry* **1996**, *35*, 16036–16047.
- (9) Yang, D.; Mok, Y.-K.; Forman-Kay, J. D.; Farrow, N. A.; Kay, L. E. *J. Mol. Biol.* **1997**, *272*, 790–804.
- (10) Denisov, V. P.; Venu, K.; Peters, J.; Hörlein, H. D.; Halle, B. J. *Phys. Chem. B* **1997**, *101*, 9380–9389.
- (11) Alexandrescu, A. T.; Rathgeb-Szabo, K.; Rumpel, K.; Jahnke, W.; Schulthess, T.; Kammerer, R. A. *Prot. Sci.* **1998**, *7*, 389–402.
- (12) Gagné, S. M.; Tsuda, S.; Spyropoulos, L.; Kay, L. E.; Sykes, B. D. *J. Mol. Biol.* **1998**, *278*, 667–686.
- (13) Dangi, B.; Blankman, J. I.; Miller, C. J.; Volkman, B. F.; Guiles, R. D. *J. Phys. Chem. B* **1998**, *102*, 8201–8208.
- (14) LeMaster, D. M. *J. Am. Chem. Soc.* **1999**, *121*, 1726–1742.
- (15) Bracken, C.; Carr, P. A.; Cavanagh, J.; Palmer, A. G. *J. Mol. Biol.* **1999**, *285*, 2133–2146.
- (16) Sari, N.; Holden, M. J.; Mayhew, M. P.; Vilker, V. L.; Coxon, B. *Biochemistry* **1999**, *38*, 9862–9871.
- (17) Zidek, L.; Novotny, M. V.; Stone, M. *Nature Struct. Biol.* **1999**, *6*, 1118–1121.
- (18) Forman-Kay, J. D. *Nature Struct. Biol.* **1999**, *6*, 1086–1087.
- (19) Lee, A. L.; Kinnear, S. A.; Wand, A. J. *Nature Struct. Biol.* **2000**, *7*, 72–77.
- (20) Cavanagh, J.; Akke, M. *Nature Struct. Biol.* **2000**, *7*, 11–13.
- (21) Brooks, C. L.; Karplus, M.; Pettitt, B. M. *Proteins: A Theoretical Perspective of Dynamics, Structure, and Thermodynamics*; John Wiley & Sons: New York, 1988.
- (22) Karplus, M.; Kushick, J. *Macromolecules* **1981**, *14*, 325–332.
- (23) Levy, R. M.; Karplus, M.; Kushick, J.; Perahia, D. *Macromolecules* **1984**, *17*, 1370–1374.
- (24) Hayward, S.; Kitao, A.; Hirata, F.; Gō, N. *J. Mol. Biol.* **1993**, *234*, 1207–1217.
- (25) Amadei, A.; Linssen, A. B.; Berendsen, H. J. *Proteins* **1993**, *17*, 412–425.
- (26) Case, D. A. *Curr. Opin. Struct. Biol.* **1994**, *4*, 285–290.
- (27) Amadei, A.; Linssen, A. B.; de Groot, B. L.; van Aalten, D. M.; Berendsen, H. J. *J. Biomol. Struct. Dyn.* **1996**, *13*, 615–625.
- (28) Hinsén, K. *Proteins* **1998**, *33*, 417–429.
- (29) Kitao, A.; Hayward, S.; Gō, N. *Proteins* **1998**, *33*, 496–517.
- (30) Abseher, A.; Nilges, M. *J. Mol. Biol.* **1998**, *279*, 911–920.
- (31) Wrabl, O. J.; Shortle, D.; Woolf, T. B. *Proteins* **2000**, *38*, 123–133.
- (32) Lienin, S. F.; Brüschweiler, R. *Phys. Rev. Lett.* **2000**, *84*, 5439–5442.
- (33) Brüschweiler, R. *J. Am. Chem. Soc.* **1992**, *114*, 5341–5344.
- (34) Palmer, A. G.; Case, D. A. *J. Am. Chem. Soc.* **1992**, *114*, 9059–9067.
- (35) Case, D. A. *J. Biomol. NMR* **1999**, *15*, 95–102.
- (36) As usual,  $|R\rangle$  denotes a column vector,  $\langle R|$  is a row vector,  $\langle R|P\rangle$  is the scalar product between  $\langle R|$  and  $|P\rangle$ , and  $|R\rangle\langle P|$  is a matrix with elements  $ij$  corresponding to the product of the  $i$ th element of  $|R\rangle$  and the  $j$ th element of  $\langle P|$ .
- (37) McQuarrie, D. A. *Statistical Mechanics*; Harper & Row: New York, 1976.
- (38) Fischer, M. W. F.; Zeng, L.; Pang, Y.; Hu, W.; Majumdar, A.; Zuiderweg, E. R. P. *J. Am. Chem. Soc.* **1997**, *119*, 12629–12642.
- (39) Lienin, S. F.; Bremi, T.; Brutscher, B.; Brüschweiler, R.; Ernst, R. R. *J. Am. Chem. Soc.* **1998**, *120*, 9870–9879.
- (40) Brooks, R. B.; Bruccoleri, R. E.; Olafson, B. D.; States, D. J.; Swaminathan, S.; Karplus, M. *J. Comput. Chem.* **1983**, *4*, 187–217.
- (41) MacKerell, A. D., Jr.; Bashford, D.; Bellott, M.; Dunbrack, R. L., Jr.; Evanseck, J. D.; Field, M. J.; Fischer, S.; Gao, J.; Guo, H.; Ha, S.; Joseph-McCarthy, D.; Kuchnir, L.; Kucera, K.; Lau, F. T. K.; Mattos, C.; Michnick, S.; Ngo, T.; Nguyen, D. T.; Prodhom, B.; Reiher, W. E., III.; Roux, B.; Schlenkerich, M.; Smith, J. C.; Stote, R.; Straub, J.; Watanabe, M.; Wiórkiewicz-Kuczera, J.; Yin, D.; Karplus, M. *J. Phys. Chem. B* **1998**, *102*, 3586–3616.
- (42) Brüschweiler, R. *J. Chem. Phys.* **1995**, *102*, 3396–3403.
- (43) Buck, M.; Karplus, M. *J. Am. Chem. Soc.* **1999**, *121*, 9645–9658.
- (44) Lienin, S. F. *Anisotropic Dynamics in Molecular Systems Studied by NMR Relaxation*; Dissertation ETH Zürich, No. 12871, 1998.
- (45) Hamm, P.; Lim, M.; Hochstrasser, R. M. *J. Phys. Chem. B* **1998**, *102*, 6123–6138.
- (46) Schneider, D. M.; Dellwo, M. J.; Wand, A. J. *Biochemistry* **1992**, *31*, 3645–3652.
- (47) Tjandra, N.; Feller, S. E.; Pastor, R. W.; Bax, A. *J. Am. Chem. Soc.* **1995**, *117*, 12562–12566.
- (48) Brüschweiler, R.; Roux, B.; Blackledge, M.; Griesinger, C.; Karplus, M.; Ernst, R. R. *J. Am. Chem. Soc.* **1992**, *114*, 2289–2302.